Electronic Supplementary Information for

Electrokinetic effect and H_2O_2 boosting in synthetic graphene/α-FeOOH aerogel films for electricity generation

Wei Wang,[a,b] Wenbin Gong,[a] Yaqiong Wang,[c] Guangyong Li,[a] Weibang Lu,[a] Yezi You[d] and Xuetong Zhang,*[a,e]

[a.] Suzhou Institute of Nano-tech and Nano-bionics, Chinese Academy of Sciences, Suzhou 215123, P.R. China. xtzhang2013@sinano.ac.cn

[b.] Nano Science and Technology Institute, University of Science and Technology of China, Suzhou 215123, P.R. China.

[c.] School of Engineering and Materials Science, Queen Mary University of London, London, E1 4NS, United Kingdom

[d.] Hefei National Laboratory for Physical Sciences at the Microscale, CAS Key Laboratory of Soft Matter Chemistry Department of Polymer Science and Engineering, University of Science and Technology of China, Hefei 230026, P.R. China

[e.] Division of Surgery & Interventional Science, University College London, London NW3 2PF, United Kingdom

Table of contents

Note 1-The decomposition of H_2O_2

As reported by other researchers, the first step in the heterogeneous reaction is the surface complexation of H_2O_2 to ≡Fe(III) forming $\equiv Fe^{III}\ H_2O_2$, leading to the formation of $HO_2\cdot$ radicals in solution, H_2O_2 decomposition is promoted in the presence of α-FeOOH. Eqs. ((1), (2), (3), (4)) [1-2]

$\equiv Fe^{III} + H_2O_2 \rightarrow \equiv Fe^{III}\ H_2O_2$ (1)

$\equiv Fe^{III}\ H_2O_2 \rightarrow \equiv Fe^{II} + HO_2\cdot + H^+$ (2)

$\equiv Fe^{III} + HO_2\cdot \rightarrow \equiv Fe^{II} + O_2 + H^+$ (3)

$\equiv Fe^{II} + H_2O_2 \rightarrow \equiv Fe^{III} + OH^+ + OH^-$ (4)

The catalytic activity of CGA by α-FeOOH might be attributed to its high surface area and mesoporous structure, which give H_2O_2 full access to the inner surfaces of the agglomerates, promoting H_2O_2 decomposition.

Note 2-Power calculation of HPG device

The maximum electrical output power of the HPG device:

$P_{max} = 0.25 V_{oc}\ I_{sc}$

where P_{max} is the maximum power, V_{oc} is the open circuit voltage and I_{sc} is the short circuit current, which occurs when the external load resistance is set equal to the internal resistance of the HPG device. P_{max} in the Equation is obtained from experimental data of potential difference, *E*, versus current, *I*. In a simple case where *E-I* curve is liner, it is easy to find that P_{max} is given by the rectangle of greatest area under the *E–I* curve.

Note 3- Simulation

Both molecular dynamics (MD) and density functional theory (DFT) simulation were performed to investigate the mechanisms of the bubbling hydrovoltaic effect in the catalytic graphene aerogel. The MD simulations were performed in the canonical ensemble at 300 K by using LAMMPS (large-scale atomic/molecular massively parallel simulator) code. The DREIDING forcefield was employed to describe the intra- and inter-molecular interactions in the H_2O and H_2O_2 solvent, while the atomic charges were calculated with the charge equilibration (QEq) method. The timestep was set to be 0.2 fs, and the MD calculations stopped until the energy variations were smaller than 0.1% to reach the equilibrium state. The DFT simulations were performed with the Vienna Ab-initio Simulation Package (VASP), using the projector-augmented wave (PAW) potentials with a plane-wave cutoff of 500 eV. The Perdew-Burke-Ernzerhof (PBE) form of the exchange-correlations functional was employed in the simulation, and the long-range interlayer van der Waals (vdW) interaction was described with DFT-D2 method. The ions were simulated by adjusting the charge neutrality level with a uniform jellium countercharge and considering dipole correction to the total energy. The systems were

fully relaxed without any constraint by using the conjugate gradient method, in which the convergence for total energy and interaction force was set to be 10^{-5} eV and 10^{-3} eV/Å, respectively.

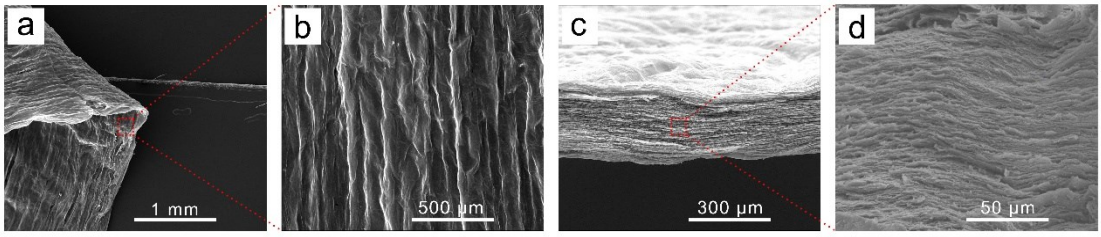

Fig.S1 Scanning electron microscopy (SEM) images of surface (a, b) and cross section (c, d) of the CGA film.

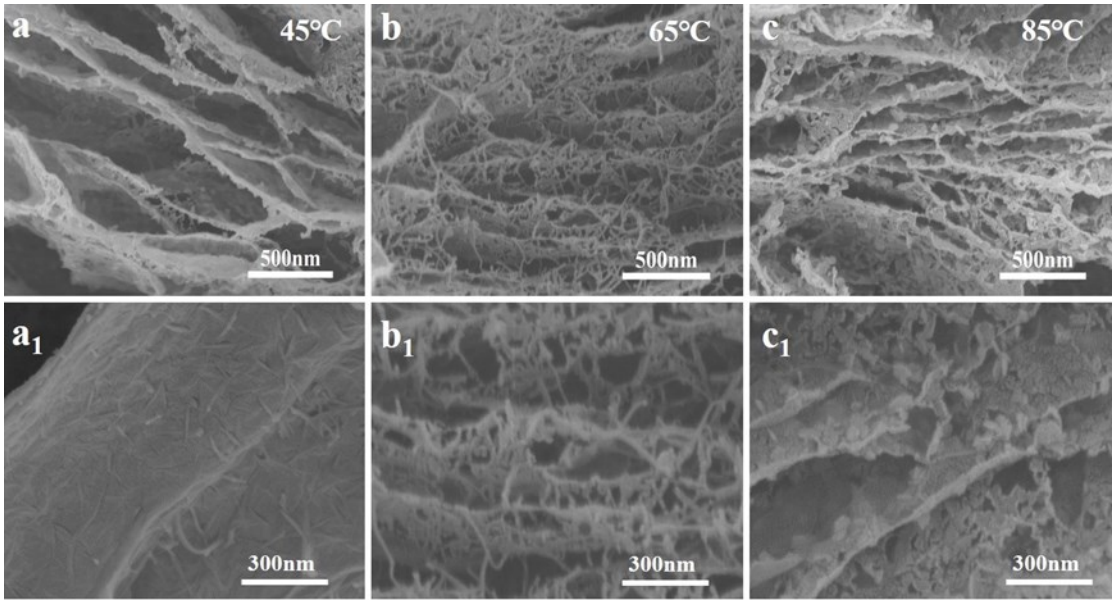

Fig.S2 SEM images of α-FeOOH/ reduced graphene oxide processed at (a) 45 °C, (b) 65 °C and (c) 85 °C. The α-FeOOH fibers are short and mainly grew along the RGO sheets at the processing temperature of 45 °C. When the temperature increased to 65 °C, the obtained α-FeOOH fibers grew much longer along and cross the RGO sheets and formed a 3-D network structure. When the temperature increased to 85 °C, the fibers agglomerated together and formed larger clusters all along the RGO sheets.

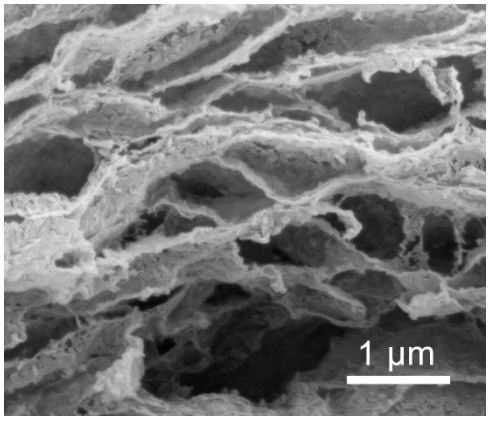

Fig.S3 The morphology of the composite aerogel (RFA) made by directly mixing of RGO and FeSO4. The RFA is obtained by directly mixing graphene oxide and $FeSO_4$, then heated still at 65 °C for 6h and washed with absolute ethanol for several times followed by supercritical drying with CO_2 (40 °C, 10 MPa) for 12 hours.

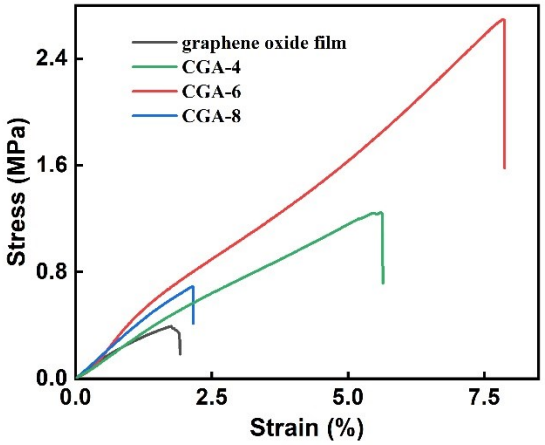

Fig.S4 Mechanical tests of CGA films. The mechanical tests showed that CGA films exhibited typical stress - strain behavior at room temperature, highlighting that the specific rivet structure of CGA-6 film brought excellent mechanical properties. The fracture strength of CGA-6 film (2.71 MPa) is 116.8% higher than CGA-4 film (1.25 MPa) and 298.5% higher than CGA-8 film (0.68 MPa), and the Young's modulus of CGA-6 film (34.74 MPa) is 55.6% higher than CGA-4 film (22.32 MPa) and 9.8% higher than CGA-8 film (31.63 MPa). And the fracture strength of CGA is greater than that of graphene oxide film.

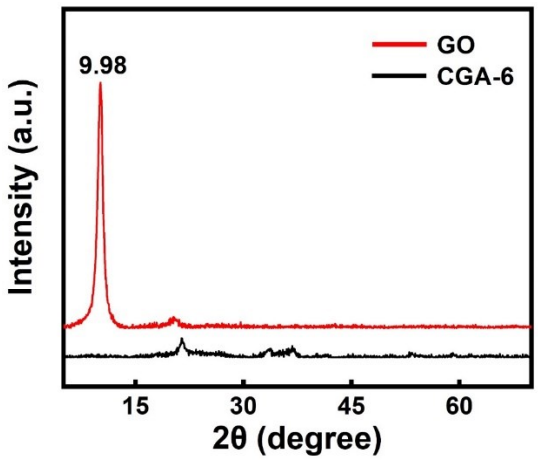

Fig.S5 XRD patterns of GO and CGA-6. For the GO, a band can be visualized at 2θ = 9.98°, which belongs to the reflection of the plane (001) characteristic of the GO. [3] The d-space of the GO is 9.05 Å. The increase in distance between the GO layers is due to the presence of functional groups in the basal planes of the material. [4] For the CGA, the XRD spectrum of α-FeOOH/RGO shows a typical pattern for α-FeOOH (more details see Fig.2p).

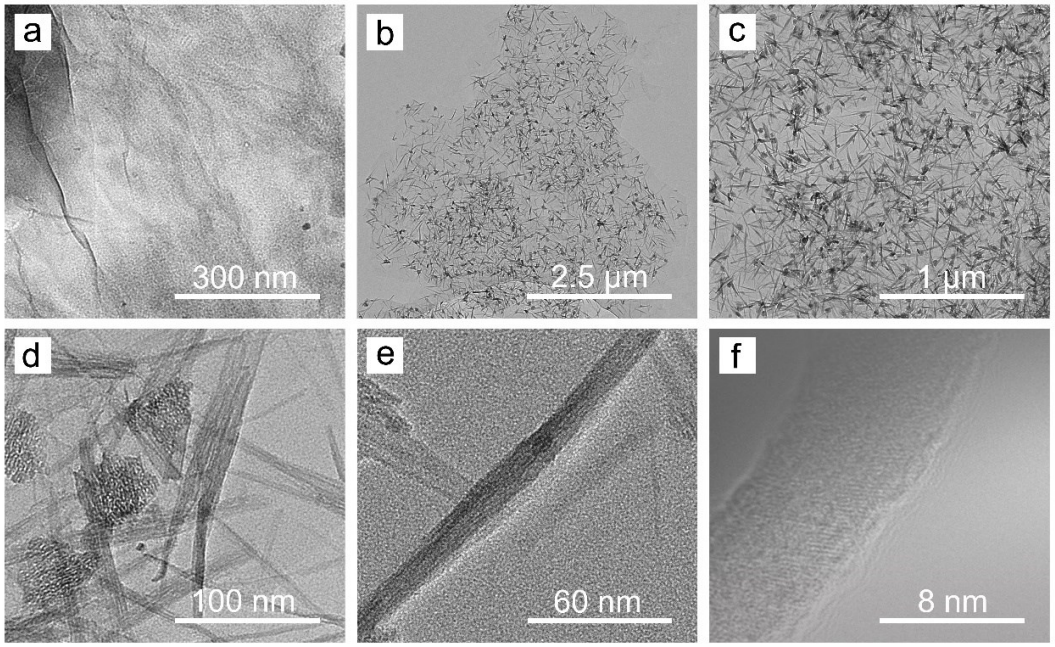

Fig.S6 Transmission electron microscope (TEM) images of GO (a) and CGA (b-f) with different magnifications.

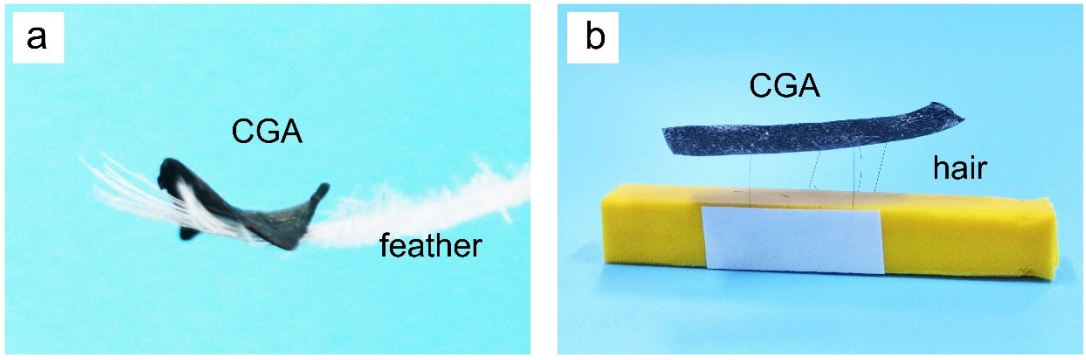

Fig.S7 A piece of CGA film can be well placed on a feather (a) and several hairs (b).

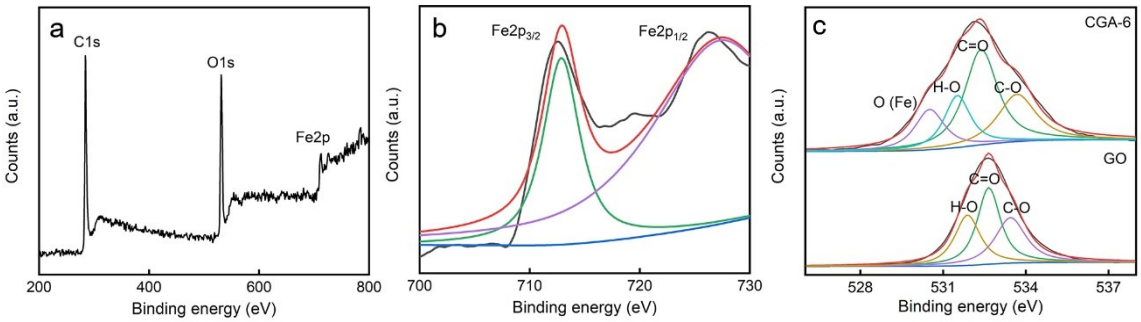

Fig.S8 X-ray photoelectron spectroscopy (XPS) spectra of CGA film: (a) full scan, (b) core-level Fe2p and (c) oxygen O1s peak. The photoelectron lines at 285 eV, 531 eV, and 711 eV in the wide-scan XPS spectrum confirmed the existence of high levels of C, O, and Fe elements in the CGA, which belong to C1s, O1s, and Fe2p respectively.

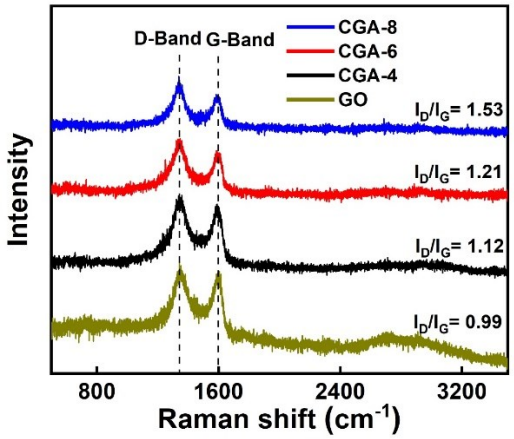

Fig.S9 Raman spectra of the CGA-4, CGA-6, CGA-8 and GO. For GO, the D-band and G-band are situated at 1346 cm^{-1} and 1596 cm^{-1} respectively, which agrees with the earlier report. [5] The D/G intensity ratio for RGO is higher compared to that of GO. The conjugated sp^2 carbon network is re-established after the chemical reduction of GO. The re-established sp^2 carbon network size is usually small compared to the original layer, leading to an increase in the D/G intensity ratio. [6]

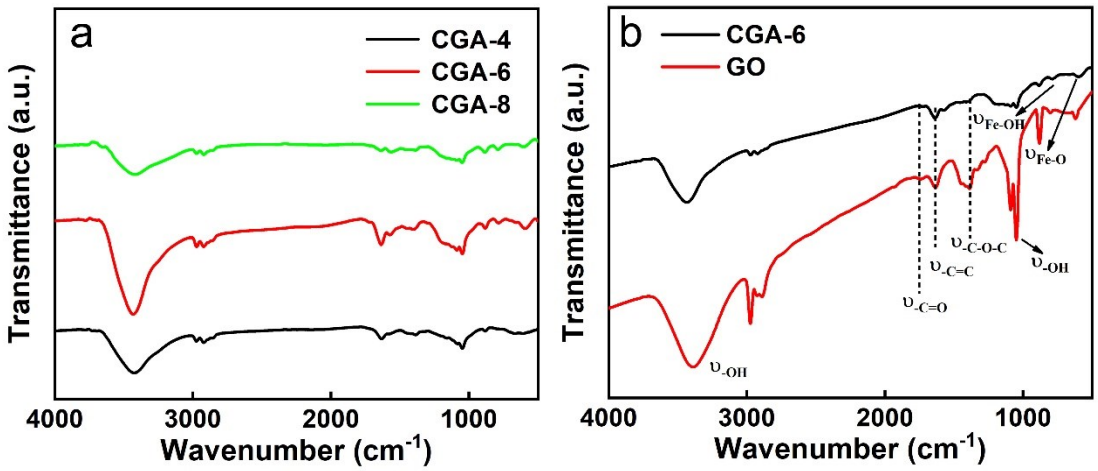

Fig.S10 The Fourier transform infrared (FT-IR) spectra of the CGA-4, CGA-6, CGA-8 and GO, the absorption bands of C=O at 1750 cm^{-1} and epoxy C-O at 1255 cm^{-1} of GO were significantly decreased, indicating that the graphene oxide layer was effectively reduced. At the same time, the two bands at 890 cm^{-1} and 795 cm^{-1} are typical bending vibrations of Fe-OH.

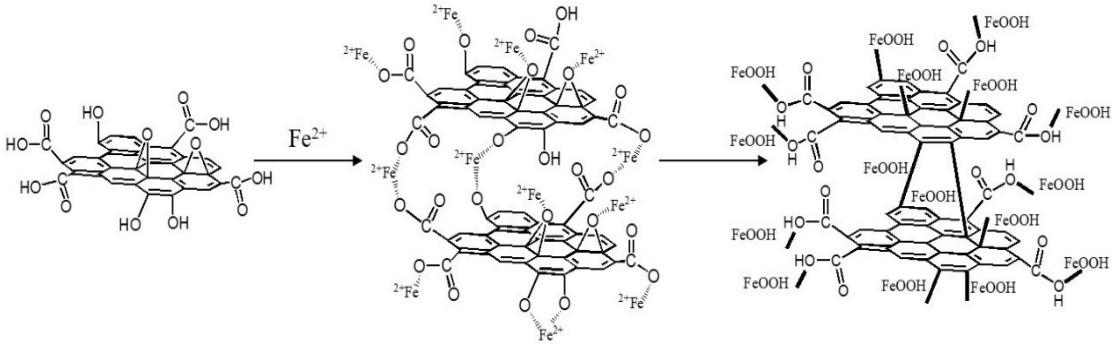

Fig.S11 Possible reaction mechanism: Fe^{2+} and GO were crosslinked through metal coordination bonds and formed a hydrogel. The epoxy functional groups on GO were reduced by Fe^{2+} with final CGA films obtained.

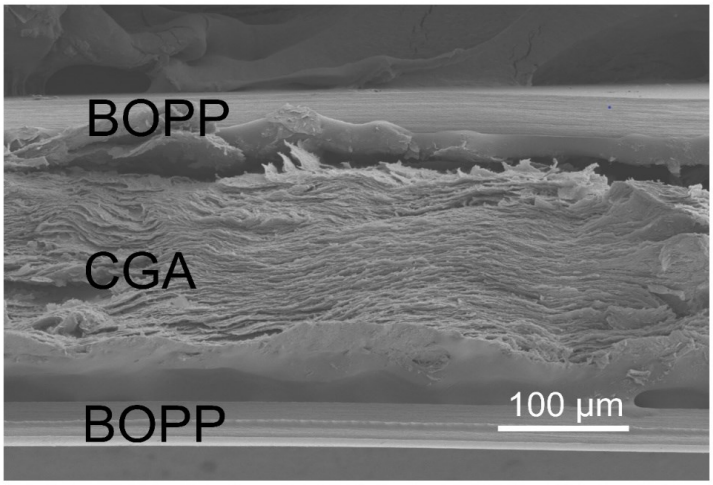

Fig.S12 The HPG device is composed of biaxially oriented polypropylene (BOPP) encapsulated CGA film like a sandwich, ensuring that the saline droplets flow properly within the film and flow inside the CGA and do not directly contact the electrodes.

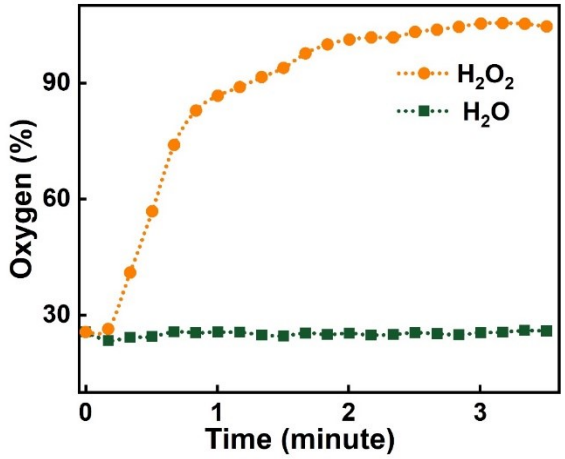

Fig.S13 The amount of oxygen produced by a drop of water droplet and a water droplet with H_2O_2

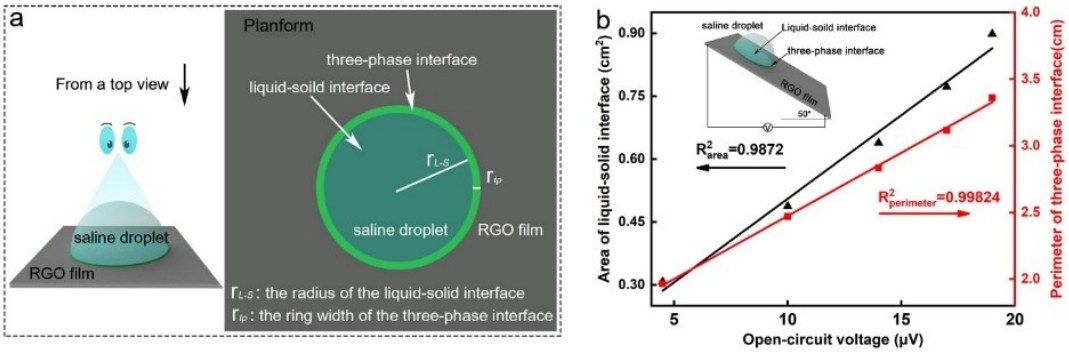

Fig.S14 There were a liquid-solid interface and a three-phase interface when a droplet was free on the surface of the RGO film. (a) The liquid-solid interface is a circle with a radius of r_{L-S}, and the three-phase interface is a ring with a ring width of r_{tp}, where r_{tp} is a small constant, so the area of the three-phase interface is mainly affected by the annular circumference of ring. (b) Multiple droplets of different volumes slide down from the same height successively, and obtain the same speed on the RGO film. The linear relationship between the open-circuit voltage of the saline droplets on the RGO film and the area of the liquid-solid interface or the perimeter of three-phase interface, indicate the open-circuit voltage is more dependent on the three-phase interface as the R^2 of the latter is closer to 1.0 than that of the former.

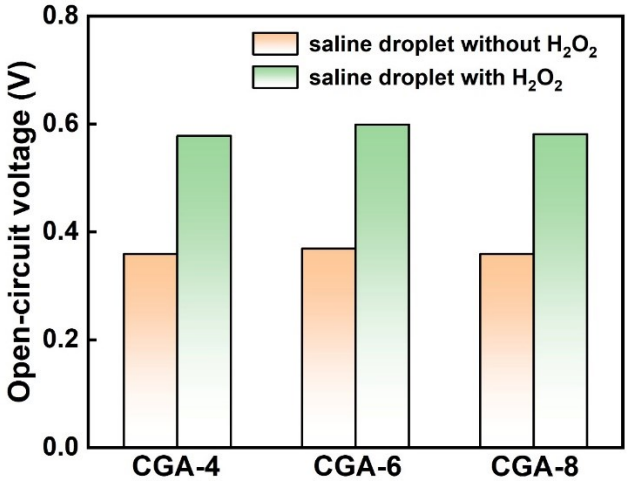

Fig.S15 The open-circuit voltage of CGA-4, CGA-6 and CGA-8 produced using a saline droplet with H_2O_2 and saline droplet without H_2O_2 (1 M NaCl).

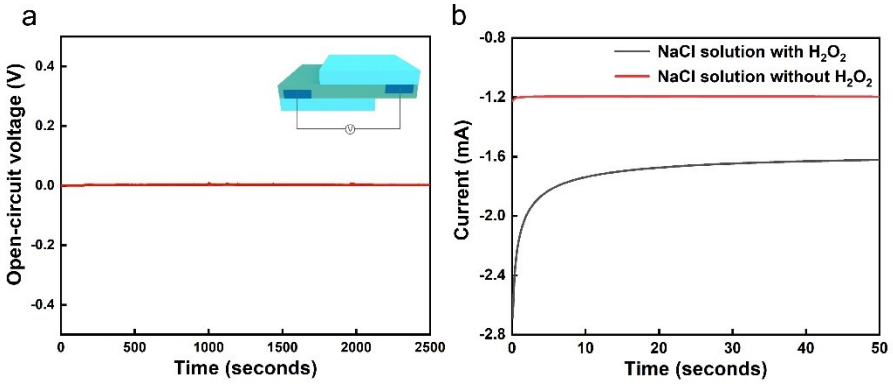

Fig.S16 (a)There was no voltage output at both ends of the CGA when the liquid was no longer flowing, (b) the short-circuit current value of HPG completely immersed in NaCl solution with H_2O_2 is 35% higher than that of NaCl solution without H_2O_2 under the constant potential of 0.7V.

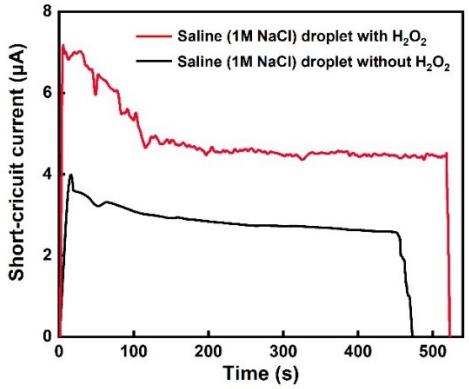

Fig.S17 The measured short-circuit current from HPG device by dropping a saline (1 M NaCl) droplet with or without H_2O_2.

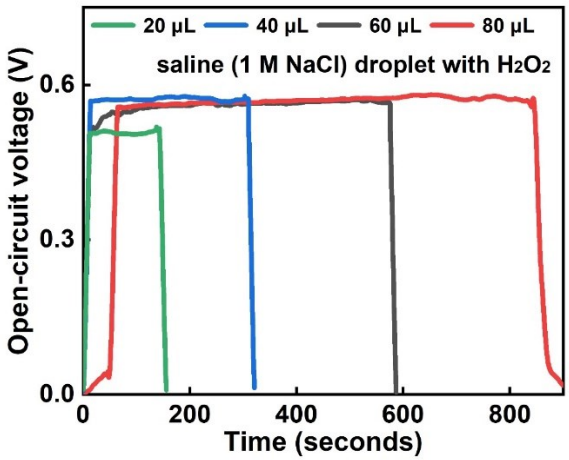

Fig.S18 The open-circuit voltage of HPG device produced using at different volumes of saline droplets with H_2O_2(20μL, 40μL, 60μL and 80μL).

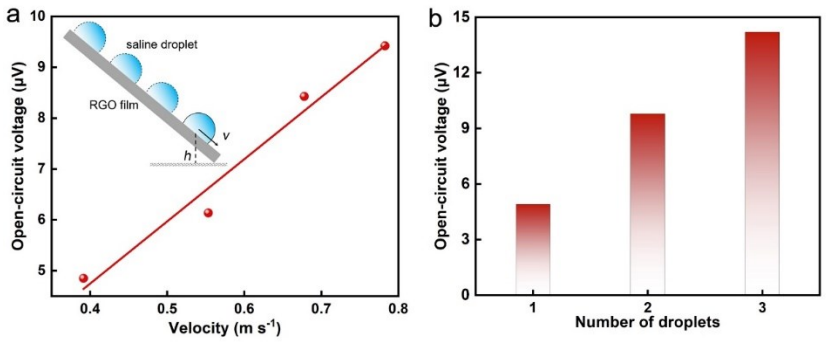

Fig. S19 (a) The saline (1M NaCl) droplets of the same volume were flowed on the RGO film at different heights to obtain different speeds, and the relationship between the open-circuit voltage at two ends of the RGO film and the flowing speed of the saline droplets was measured, and the relationship between the different speeds of saline droplet movement and the voltage output was tested and the result showed that the greater the speed, the greater the open-circuit voltage. (b) Different numbers of saline (1M NaCl) droplets of the same volume were flowed on the RGO film at the same height to obtain the same speed, and the relationship between the open-circuit voltage at two ends of the RGO film and the number of saline droplets was measured, and the results showed that the number of droplets was proportional to the voltage.

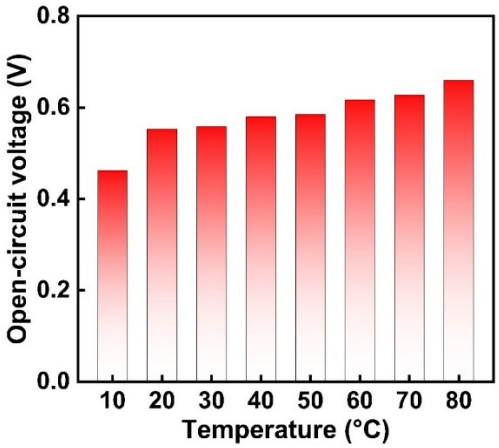

Fig.S20 Effects of ambient test temperature on the open-circuit voltage of HPG device. The test ambient temperature of HPG device affects the open-circuit voltage with saline droplet (0.1 M NaCl) with H_2O_2; With the increase of temperature of the whole device, the open-circuit voltage showed a trend of increasing gradually.

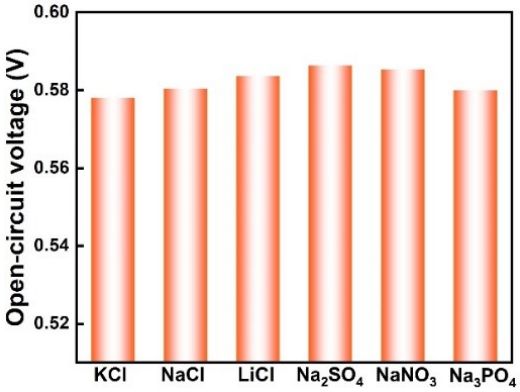

Fig.S21 The influence of different ions on open-circuit voltage and results show that solutions with different ions can generate voltage and have almost the same effect as that of NaCl.

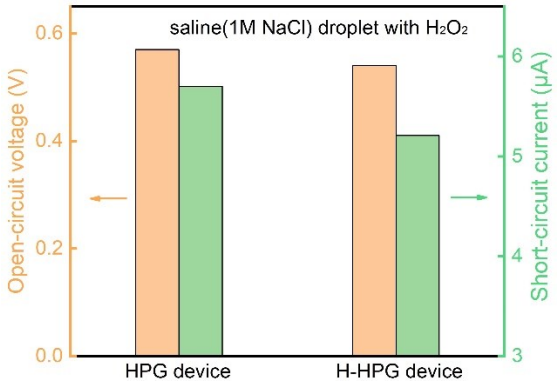

Fig.S22 The open-circuit voltage of HPG device and H-HPG device (It is assembled by CGA after heating at 600℃ for 1h.) produced using a saline droplet without H_2O_2 (1 M NaCl).

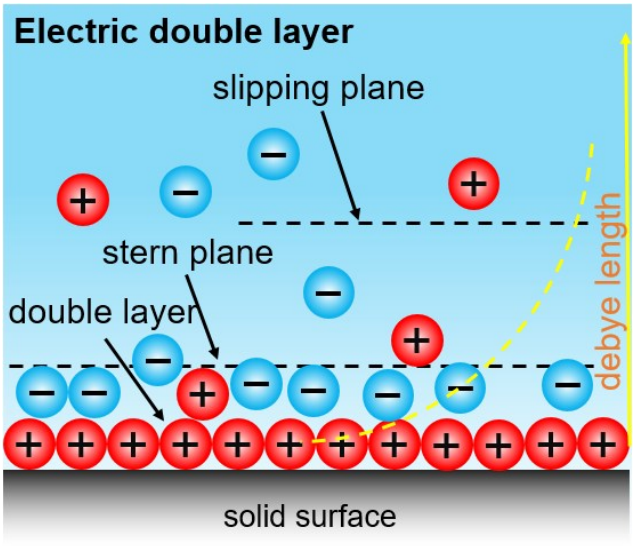

Fig.S23 Since the current is generated inside the electric double layer, this phenomenon is limited within the thickness of the electric layer, that is, the debye length (λ_D), which can be calculated as[7]

$$\lambda_D = \sqrt{\varepsilon\varepsilon_0 k_B T / 2 n_{bulk} z^2 e^2}$$

where ε is the dielectric constant of water, ε_0 is the permittivity of vacuum, k_B is the boltzmann constant, T is the absolute temperature, n_{bulk} is the bulk ion concentration, z is the valence of the ions, and e is the charge of an electron. The formula tells us that the debye length of the ion is inversely proportional to the square of the ion concentration, that is, in the high ion concentration system, the anion has a shielding effect on the cations forming the electric double layer.

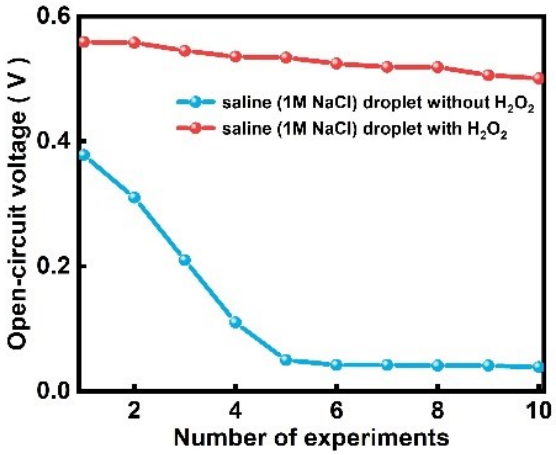

Fig.S24 The relationship between the number of device performance and the open-circuit voltage by saline (1M NaCl) droplet with or without H_2O_2. The saline (1M NaCl) droplets with H_2O_2 can make the open-circuit voltage more stable.

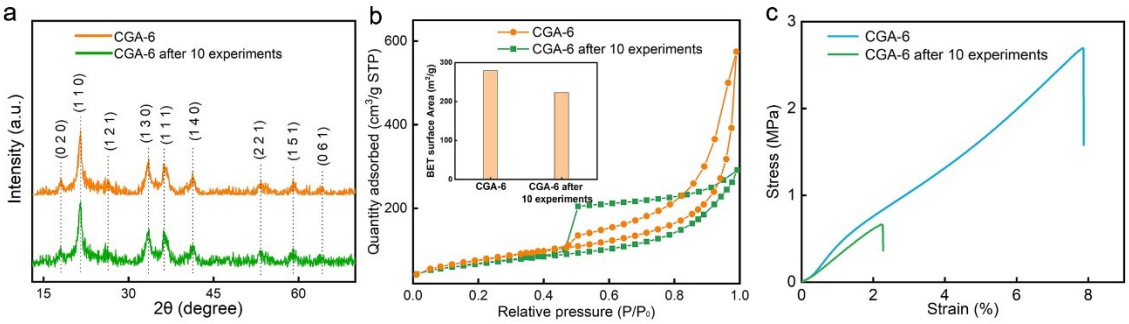

Fig.S25 (a) X-ray diffraction (XRD) patterns of CGA-6 and CGA-6 after 10 experiments. (b) Nitrogen adsorption−desorption isotherms of CGA-6 and CGA-6 after 10 experiments. The insets are their specific surface area values. (c) The fracture strength of CGA-6 and CGA-6 after 10 experiments.

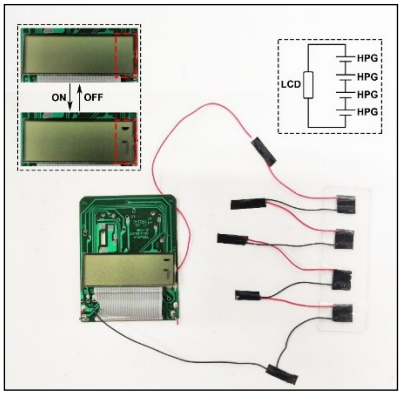

Fig.S26 Four assemblies of HPG in series can light a specific symbol when connecting to a liquid crystal display (LCD).

References

1 F. Xiao, W. Li, L. Fang and D. Wang, *J. Hazard. Mater.,* 2016**, 308**, 11-20.

2 M. C. Lu, J. N. Chen and C. P. Chang, *J. Hazard. Mater.,* 1999**, 65**, 277-288.

3 P. Bradder, S. K. Ling, S. Wang and S. Liu, *J. Chem. Eng. Data,* 2011**, 56**, 138-141.

4 H. Xu, Z. Hu, A. Lu, Y. Hu, L. Li, Y. Yang, Z. Zhang and H. Wu, *Mater. Chem. Phys.,* 2013**, 141**, 310-317.

5 Y. Zhang, L. Chen, Z. Xu, Y. Li, B. Zhou, M. Shan, Z. Wang, Q. Guo, and X. Qian, *Mater. Lett.,* 2012**, 89**, 226-228.

6 K. Satheesh and R. Jayavel, *Mater. Lett.,* 2013, **113**, 5-8.

7 J. Yin, X. Li, J. Yu, Z. Zhang, J. Zhou and W. Guo, *Nat. Nanotechnol.*, 2014, **9**, 378-383.